POLITECNICO DI TORINO
Repository ISTITUZIONALE

Use of microreactors and freeze-drying in the manufacturing process of chitosan coated PCL nanoparticles

Original
Use of microreactors and freeze-drying in the manufacturing process of chitosan coated PCL nanoparticles / Zelenková, T.; Onnainty, R.; Granero, G. E.; Barresi, A. A.; Fissore, D.. - In: EUROPEAN JOURNAL OF PHARMACEUTICAL SCIENCES. - ISSN 0928-0987. - STAMPA. - 119:(2018), pp. 135-146. [10.1016/j.ejps.2018.04.006]

Availability:
This version is available at: 11583/2741882 since: 2020-02-02T19:32:38Z

Publisher:
Elsevier

Published
DOI:10.1016/j.ejps.2018.04.006

Terms of use:

This article is made available under terms and conditions as specified in the corresponding bibliographic description in the repository

Publisher copyright
Elsevier postprint/Author's Accepted Manuscript

© 2018. This manuscript version is made available under the CC-BY-NC-ND 4.0 license http://creativecommons.org/licenses/by-nc-nd/4.0/.The final authenticated version is available online at: http://dx.doi.org/10.1016/j.ejps.2018.04.006

(Article begins on next page)

12 October 2024

European Journal of Pharmaceutical Sciences [ISSN: 0928-0987], 2018, 119, 135-146.

DOI: 10.1016/j.ejps.2018.04.006

Use of microreactors and freeze-drying in the manufacturing process of chitosan coated PCL nanoparticles

Tereza Zelenková[1], Renée Onnainty[1,2], Gladys Ester Granero[2], Antonello A. Barresi[1], Davide Fissore[1,*]

1. Dipartimento di Scienza Applicata e Tecnologia, Politecnico di Torino,

Corso Duca degli Abruzzi 24, 10129 Torino, Italy

2. Departamento de Ciencias Farmacéuticas, Facultad de Ciencias Químicas, Universidad Nacional de Córdoba,

Av. Medina Allende y Haya de la Torre, Córdoba, Argentina

* *Corresponding author*
email: davide.fissore@polito.it
tel: 0039-011-0904693

Abstract

This paper is focused on the synthesis of chitosan-coated polycaprolactone nanoparticles in microreactors and on the freeze-drying of the nanosuspension, to separate the particles from the liquid phase. Nanoparticles were produced in the confined impinging jets mixer (CIJM) and in the multi-inlet vortex mixer (MIVM), using the solvent displacement method, with acetone or *tert*-butanol (TBA) as polymer solvent. The study was initially carried out considering a feed flow rate of 80 ml/min: using acetone, the mean particle size was lower (163±7 nm) and the Zeta potential was higher (31.4±37 mV) with the MIVM, with respect to the CIJM (265±31 nm and 9.8±2.4 mV, respectively). Slightly larger particles were obtained using TBA in the MIVM (mean diameter: 221±44 nm): in this case it is no longer required removing the solvent before the freeze-drying stage. The effect of the liquid flow rate was then investigated, confirming that the best results were obtained at 80 ml min^{-1}. With respect to the freeze-drying process, the effect of lyoprotectants and of steric stabilizers on particle stability was investigated. Best results were obtained with 5% sucrose and 2.5% Poloxamer 388 (mean diameter: 306±8 nm); in all cases Zeta potential remained positive and larger than +30 mV. Preliminary results about the encapsulation of a test drug, ciprofloxacin, are also shown and discussed.

Keywords

Nanoparticles; nanotechnology; solvent displacement; chitosan; freeze-drying; confined impinging jets mixer; multi-inlet vortex mixer.

Introduction

Chitosan coated nanoparticles have attracted a lot of interest in recent years, as the presence of chitosan can strongly improve the nanoparticles mucoadhesive properties. In fact, chitosan may interact with the negatively charged (at the physiological pHs) mucosal surfaces and it is also capable of opening the junctions between mucosal cells, thus facilitating the transport of drugs through the epithelia (Lehr et al., 1992; Issa et al., 2005; Andrews et al., 2009; Dash et al., 2011). Therefore, coating drug containing nanoparticles, constituted by natural (e.g. polysaccharides and proteins, as albumin and gelatin) or synthetic polymers, with chitosan allows obtaining the drug delivery directly to the mucosal tissue (Huang et al., 2000; Chowdary and Rao, 2004; Andrews et al., 2009).

Polycaprolactone (PCL) is one of the polymers most commonly used in this case due to its biodegradability, biocompatibility, non-mutagenicity and non-toxicity. Moreover, its biodegradation products formed in the intestinal lumen can be easily removed from the body through metabolism or absorption (Wu et al., 2000). Finally, with respect to the cost, the PCL is significantly cheaper than other polyesters (e.g. polyglycolide and polylactide).

Gupta et al. (2011) investigated the use of chitosan in such a way, finding out that chitosan coated PCL nanoparticles could effectively be used for immunization against influenza when they are administrated through the nasal route. Mazzarino et al. (2012) obtained polycaprolactone nanoparticles covered with chitosan to deliver curcumin across the buccal route. The release of ovalbumin, bovine serum albumin and human insulin loaded in nanoparticles composed of chitosan and tripolyphosphate was investigated by Rampino et al (2013). Besides, chitosan exhibits other important characteristics that makes it particularly suitable for nanoparticles production: it is in fact biodegradable (Lee et al., 1995), and it has good immune stimulating characteristics (Nishimura et al., 1986).

Several bottom-up methods, e.g. emulsification-evaporation (Nagavarma et al., 2012),

emulsification–diffusion (Mersmann, 1999; Merisco-Liversidge et al., 2003; Nagavarma et al., 2012) and solvent displacement (Fessi et al., 1989; Horn and Riegen, 2001), are generally used to produce nanoparticles in the pharmaceutical industry. They require dissolving the reactants into adequate solvents, followed by a precipitation (or condensation) stage to form the nanoparticles. Among these methods, the solvent displacement offers several advantages with respect to the others: it allows obtaining small size nanoparticles, and varying their size and distribution by modifying the operating conditions. This method has the advantage of being cheap and it allows obtaining highly reproducible nanoparticle sizes by using solvents with low toxic potential (e.g. acetone, *tert*-butanol, tetrahydrofuran) (Horn and Rieger, 2001; Lince et al., 2008; Barresi et al., 2015). At first the polymer is dissolved into a solvent wherein it has a good solubility; then, this solution is mixed with an anti-solvent, i.e. a liquid where the polymer is insoluble: nanoparticles are obtained through precipitation (Horn and Rieger, 2001; Di Pasquale et al., 2012).

Several solvents may be used to dissolve PCL, as listed by Bordes et al. (2010). Acetone was one of the first solvents used for nanoparticles synthesis through the solvent displacement method. Fessi et al. (1989) employed it in the production of poly(D,L-lactide) nanoparticles, and, then, it was extensively used for nanoparticles production (see, among the others, Peracchia et al., 1998; Lince et al., 2008; Lince et al., 2011a; Zelenková et al., 2014, 2015, 2017). After the synthesis process, acetone has obviously to be removed from the nanoparticles suspension, e.g. through evaporation, at low pressure (and, thus, low temperature) to avoid jeopardizing nanoparticles characteristics and, finally, water can be removed through freeze-drying in order to improve the nanoparticles long-term stability. As an alternative, *tert*-butyl alcohol (TBA) was proposed as PCL solvent in the manufacturing process (Zelenková et al., 2015). The interest toward this solvent is due to the fact that it is possible to freeze-dry the nanoparticles suspension without removing the solvent because of

the high freezing point of the solvent (24°C). Besides, the vapor pressure of TBA is quite high and its toxicity is very low. Finally, TBA can accelerate significantly the drying process as its presence in the aqueous system results in the formation of large needle-shaped crystals in the freezing stage: after the sublimation of ice crystals a highly porous cake is obtained, resulting in a faster drying process (Kasraian and DeLuca, 1995; Wittaya-Areekul and Nail, 1998; Teagarden and Baker, 2001; Ni et al., 2001; Pisano et al., 2014).

The stream containing the polymer and that with the anti-solvent have to be rapidly and effectively mixed in such a way that nanoparticles with the desired mean size and size distribution are obtained. The confined impinging jets mixer (CIJM) can be effectively used to this purpose (Johnson and Prud'homme 2003a, 2003b; Lince et al., 2008, 2009, 2011b, 2011c; Zelenková et al., 2014, 2015): the device consists of a small chamber where the two streams are fed at high velocity, so that a rapid mixing is obtained, as investigated through computational fluid dynamics by Marchisio et al. (2006), Gavi et al. (2007), Lince et al. (2011c), Di Pasquale et al. (2012), Barresi et al. (2015). As an alternative, the multi inlet vortex mixer (MIVM) was also proposed. Unlike the CIJM, in the MIVM the two feeds enter the reactor tangentially, thus creating a vortex in the mixing chamber (Liu et al., 2008a; Marchisio et al., 2008, 2009). Besides, it is also possible to feed other two streams, adding several degrees of freedom to the system. For example, Liu et al. (2008b) used the MIVM to produce bifenthrin nanoparticles by using one stream with the bifenthrin dissolved in THF, the second stream consisting of PVP and PVOH in water (or of PAA-b-PBA in methanol), and the other two streams containing water. Shen et al. (2011) used the MIVM to produce various polymeric nanoparticles containing β-Carotene and polyethyleneimine, and insulin/ tripolyphosphate/chitosan nanoparticles were also produced in a MIVM by He et al. (2017).

Once the nanoparticles suspension has been obtained, water has to be removed to safe store them: in fact, by this way it is possible to avoid nanoparticles aggregation, drug escape

from nanoparticles, and the degradation of the polymers constituting the nanoparticles. The freeze-drying process is the preferred route to get this result (Abdelwahed et al., 2006a, 2006b, 2006c; Beirowski et al., 2011a, 2011b, 2011c) due to the low operating temperatures. Several excipients are required in the formulation to preserve the particle size distribution in the freeze-drying process: monosaccharides (e.g. glucose), disaccharides (e.g. sucrose, threhalose) and their derivates (mannitol), dextran, polyvinylpyrrolidone, and others are quite often used for this purpose. In the freezing stage, at a certain temperature, these molecules form a glassy matrix where nanoparticles can be entrapped and, thus, protected against the mechanical stress related to the growth of the ice crystals ("vitrification hypothesis", Pikal, 1999). In this framework, when mannitol is used the particle size is hardly preserved, mainly due to the mannitol crystallization in the freezing stage (Zelenková et al., 2014; Barresi et al., 2015); nevertheless, in case other molecules are also used, mannitol crystallization is avoided, and the stability of the nanoparticles is preserved (Abdelwahed et al., 2006a; Zelenková et al., 2014). Aiming to avoid particle aggregation during the freeze-drying process, steric stabilizers have to be added to the suspension. These molecules are adsorbed onto the surface of the nanoparticles (by means of hydrogen bonds), and this allows avoiding the aggregation of the particles ("water replacement theory", Crowe et al., 1993). Polymers and surfactants like Cremophor EL, a nonionic surfactant composed by oxylated triglycerides of ricinoleic acid (Gelderblom et al., 2001), Poloxamer 388, an amphiphilic nonionic block polymer consisting of hydrophilic ethylene oxide and of hydrophobic propylene oxide (Dumortier et al., 2006), polyvinyl alcohol, and Tween 80 were demonstrated in the past to be effective for this purpose. However, the optimal stabilizer and its concentration have to be experimentally determined, because nanoparticles characteristics depend on these factors (Barresi et al., 2015).

This paper aims investigating the synthesis of PCL-chitosan nanoparticles in micro-

reactors, considering both the CIJM and the MIVM, and their recovery through freeze-drying. The effect of the flow rate of the stream containing PCL and of that containing chitosan, both in the CIJM and in the MIVM, on the mean particle size and on the Zeta potential has been investigated by means of an extended experimental investigation. Afterwards, the effect of lyoprotectants and of steric stabilizers on particle stability after a freeze-drying process was studied, focusing on the nanosuspensions produced using TBA as solvent. The paper is structured as follows: at first, the experimental methods used for particle synthesis and characterization are described, as well as the methods used for carrying out the freeze-drying experiments. The goal of the research is to produce small size particles, exhibiting positive Zeta potential: by this way the nanoparticles can be used as drug carriers for mucosal delivery. In this framework it is necessary to identify which is the optimal size range for the particles produced, that is obviously dependent on the route of administration. He et al. (2017) showed that nanoparticles with a size ranging from 50 to 100 nm exhibits the optimal performance for trans-epithelial transport, while Hickey et al. (2015) pointed out that nanoparticles whose size ranges from 100 to 500 nm exhibit the highest level of uptake in case of mucosal administration. Results are then presented and commented, and some conclusions about the optimal operating conditions for the manufacturing process of the PCL-chitosan nanoparticles are presented.

Finally, it has to be pointed out that the study whose results are presented and discussed in this paper is the first step of the development of a polymer-based drug carrier for pharmaceutical applications. In fact, we focused on the various stages of the manufacturing process, without considering any specific drug, although, as discussed by various authors (e.g. Johnson and Prud'homme, 2003a), the drug and the polymer may precipitate together, thus affecting some of the particles characteristics investigated in this paper (mean size, size distribution, zeta potential). Anyway, quite often the presence of the drug can be neglected, in

particular when the drug is entrapped in the polymeric matrix, as in this case it does not affect significantly the final mean particle size, as outlined, among the others, by Chawla and Amiji (2002). Some preliminary results obtained with an antibiotic, ciprofloxacin, are presented and discussed at the end of the paper, and they seem to confirm this statement. The interest towards ciprofloxacin is due to the fact that it is a broad-spectrum antibiotic, systematically used in several microbial contaminations such as pulmonary, urinary tract and dermal infections, as well as in conjunctivitis (Blondeau, 2004) and ocular infections (Wilhelmus et al., 2003). As this drug has a poor water solubility, that limits its oral bioavailability, it is an excellent candidate for being delivered through polymeric nanoparticles.

Materials and method

Reactants

Nanoparticles were produced using the solvent displacement method. Acetone (HPLC grade), or *tert*-butanol (anhydrous, >99.0%), depending on the goal of the experiment, was used as solvent for the PCL, while micro-filtered water (prepared with a Millipore system, Milli-Q RG, Darmstadt, Germany) was used as antisolvent. Low molecular weight PCL (14,000 Da) was used for the study. At the beginning of the process, the PCL needs to be dissolved into the solvent: its dissolution in acetone is very easy while, when the TBA was involved, it was necessary to warm up the solution at about 35°C for 30 minutes to get the complete dissolution of the PCL. Aiming to control the size of the produced nanoparticles, it was necessary to use a surfactant. In this work, the Poloxamer 388 (PEG–PPG–PEG Pluronic F-108) was used for this purpose, and it was dissolved in the water stream. Low molecular weight chitosan (deacetylation percentage: 75-85%; molecular weight ranging from 50,000 to 190,000 Da) was used in all the experiments. It was dissolved into the water stream in the presence of 1% of acetic acid (HPLC grade). The following reactants concentrations were

selected to carry out the tests: PCL (5 mg ml^{-1}), Poloxamer 388 (2.5 mg ml^{-1}) and chitosan (2.5 mg ml^{-1}), on the basis of a previous study where the effect of the concentration of the various reactants was investigated (Zelenková et al., 2018). In the tests carried out in presence of the drug, pure ciprofloxacin, with an assay ≥ 98% (HPLC based), was used: it was dissolved into the water stream containing Poloxamer 388, in the presence of 1% of acetic acid (HPLC grade). All reactants involved in the study were purchased from Sigma Aldrich (Steinheim, Germany) and used as received.

Nanoparticles synthesis

Nanoparticles synthesis was carried out both in the CIJM and in the MIVM. Figure 1 (graph A) shows the confined impinging jets mixer used in this study. It has a cylindrical mixing chamber (5 mm diameter, 11.2 mm total chamber height), with two inlet pipes (1 mm diameter). The multi inlet vortex mixer used in this study is also shown in Figure 1 (graph B). In this case, the mixing chamber has a diameter of 4 mm (with a chamber height of 1 mm), and the four inlet pipes are 1 mm diameter. Reactants are fed to the reactors by means of a syringe pump (KDS200 by KD Scientific, Holliston, USA) and using plastic syringes, 100 ml volume each. As each pump may host two syringes, when using the CIJM for particles synthesis just one pump is required, while two pumps are needed in the experiments involving the MIVM. In the tests with the CIJM, the two solutions (solvent + PCL and antisolvent + Poloxamer 388 + chitosan + acetic acid) were fed using the two inlet pipes, one for each solution, while in the MIVM different feeding conditions were tested, as described in Table 1. The aim was to investigate if feeding configuration can affect in any way the features of the produced nanoparticles, as it was shown by Liu et al. (2008a) that each stream contributes independently to the mixing in the chamber.

The ratio between the flow rate of water and that of acetone (W/A) is a parameter that

can strongly affect both mixing conditions and turbulence intensity, as it was extensively investigated in the past (Lince et al., 2008). Mathematical simulation of the behaviour of the CIJM through CFD (Computational Fluid Dynamics) evidenced that mixing efficiency is reduced when W/A is increased (Lince et al., 2011b). Thus, as it was evidenced that it is preferable that the two streams have the same momentum to reduce bypass and fluid unmixedness (Valente et al., 2012), the experimental investigation was carried out considering W/A = 1, and this parameter was not considered in the design of experiments. Similarly, in the experiments with the MIVM the same flow rate value was used for all the streams for the same reasons (Liu et al., 2008a).

The nanosuspensions produced in the CIJM are diluted in a certain amount of micro-filtered water ("quench"), gently stirred, with the goal of avoiding particle aggregation (Zelenková et al., 2014, 2015). The quench volumetric ratio used in this study, i.e. the ratio between the quantity of water used for producing the nanoparticles and that for quench, is equal to one. This value was selected on the basis of previous studies (Zelenková et al., 2014, 2015, 2017). For the experiments carried out with the MIVM no quench was carried out, as it was assumed that the dilution occurring in the mixing chamber, due to the higher amount of water fed to the reactor, could be sufficient to avoid particle aggregation and Ostwald ripening.

Finally, in the tests carried out with acetone, the solvent was removed after quenching through evaporation, by using a rotative evaporator (Stuart Rotary Evaporators, Bibby Scientific Ltd., UK); 15 minutes were required for a 4 ml sample.

Some tests were also carried out with a drug (ciprofloxacin) to investigate its effect on particle size and zeta potential. The MIVM, with TBA as polymer solvent, was used. This was due to the fact that this reactor-solvent configuration was demonstrated, in the first part of the study, to provide best results in terms of particle size, beside of shortening the duration of

the whole process ad the solvent evaporation before freeze-drying is not required. In this case ciprofloxacin was dissolved into the water stream (containing also Poloxamer 388), in presence of 1% of acetic acid.

Nanoparticles characterization

Dynamic Light Scattering (DLS) was thus used to measure the particle size distribution and, thus, the mean size of the nanoparticles, using a DLS Zetasizer Nanoseries ZS90 (Malvern Instrument, UK). Before each measurement, the sample was diluted in water (1:100) and the measure was repeated three times. The particle size distribution was determined using the Mie theory, assuming a product absorption equal to 0.010 and a product refractive index equal to 1.570. Several techniques, e.g. electron microscopy, dynamic light scattering, and many others are available for particles characterization, depending on the property of interest. In particular, the electron microscopy-based techniques can be used to determine the size, shape and surface morphology, through the direct visualization of the nanoparticles, but they provide limited information about the size distribution and the mean particle size (see, among the others, Jores et al., 2004), and DLS is the most frequently used technique for accurate estimation of the particle size and size distribution (see, among the others, DeAssis et al., 2008).

The Zeta potential was measured using the same apparatus, but with a special cell containing two electrodes. The system allowed measuring the electrophoretic mobility and, the Zeta potential was calculated using the Henry equation, with the approximation of Smoluchowsky. This is an indirect measure of the surface charge (Otsuka et al., 2003), generally used to estimate stability of a colloidal material, like the suspension of nanoparticles

Freeze-drying of nanosuspensions

After synthesis, and before freeze-drying, lyoprotectants and/or steric stabilizers were added to the nanosuspension. Sucrose and mannitol were the lyoprotectants selected in this study, while Poloxamer 388 and Cremophor EL were the steric stabilizers used. All reactants were purchased by Sigma Aldrich (Steinheim, Germany) and used as received.

With respect to the concentration of the various additives, two different studies were performed. The first study was a classic 2^2 factorial design of experiments, aiming to assess how the lyoprotectant percentage in the formulation (factor A) and the steric stabilizer percentage in the formulation (factor B) affect the mean size of the particles. High (+) and low (-) values of both parameters (factor A: 2.5 and 5% w/w and factor B: 2.5 and 5 % w/w) were considered, as it is summarized in Table 2. In this study, the total solutes concentration in the samples before freeze-drying was variable, ranging from 5% w/w to 10% w/w (in any case, all the suspensions considered in this study contained still some amount of the Poloxamer introduced in the synthesis stage). Aiming to check the correctness of the results obtained through the statistical approach, the freeze-drying study was repeated considering different concentrations in such a way that the total concentration of the solutes remained the same, and equal to 5%, as shown in Table 3.

1.5 ml of the prepared nanosuspensions were poured into DIN 58378-AR10 screw neck tubing vials (external diameter 18±0.25 mm, wall thickness of 1.2±0.06 mm). Vials were then loaded onto the shelves of a lab-scale freeze-dryer (LyoBeta 25 by Telstar, Terrassa, Spain): this device has a 0.2 m^3 drying chamber, with 4 heating shelves (0.5 m^2 is the total area available for the product), a capacitive pressure sensor (Baratron 626A by MKS Instruments, Andover, MA, USA) and T-type miniature thermocouples (Tersid, Milano, Italy). In each test 50 vial were filled with the nanosuspension that had to be investigated, and about 200 empty vials were placed around them aiming to minimize the effect of the radiative flux from chamber walls.

With respect to the operating conditions, the temperature of the heating shelf was decreased at 1°C/min from the room temperature (about 20°C) until reaching the value of -40°C, and then maintained at that value for about 5 hours (the total duration of the freezing stage was 6 hours). Then, the temperature of the shelf was increased to -20°C for 22 hours, with a chamber pressure of 0.05 mbar, in such a way that ice was removed by sublimation (primary drying). Secondary drying was carried out for 6 hours at 20°C and 0.05 mbar. Figure 2 shows the evolution of product temperature in two vials in one of the freeze-drying cycles carried out in this study: their trend is representative of those observed in all the other cycles of this study. It is possible to see that product temperature is about 20°C at the beginning of the process and, then, it decreases until about -40°C is reached. After about 6 hours, when the operating conditions are modified to allow ice sublimation, product temperature increases with the usual trend observed in freeze-drying process. After about 12-16 hours from the onset of the primary drying stage the temperature reaches a steady state value, close to the temperature of the heating shelf: this means that ice sublimation is completed as the heat provided to the product is no longer used for ice sublimation, but it is used to heat the dried product. In this case a value higher than the temperature of the heating shelf is reached due to radiation effect from the top tray. The mean value of the sublimation flux is therefore ranging from (about) 0.4 to 0.6 kg $h^{-1}m^{-2}$, and it is thus in good agreement with the values usually obtained in a freeze-drying process for pharmaceuticals. The total duration of the primary drying stage was set at 22 hours, aiming to provide an adequate extra time to complete the drying in all the vials of the batch. As the goal of the study was not the optimization of the drying process, we did not evaluate the limit temperature of the different formulations (using either DSC or freeze-drying microscopy), using this value for in-line or off-line optimization, but we selected the operating conditions on the basis of a previous study (Zelenková et al., 2014, 2015), focusing on the effect of the lyoprotectants on final product quality. In any case,

according to the temperature profiles measured, ice sublimation was considered completed at the end of the primary drying stage, and at the end of the whole drying process a good cake appearance was observed, without any significant evidence of shrinkage or collapse of the dried product, that are generally undesired at the end of the drying process. Micro-collapse, i.e. a small-scale collapse resulting in the formation of small holes in the dried cake could have occurred during the drying stage, but this phenomenon is in general responsible for a lower resistance of the dried cake to mass transfer (from the interface of sublimation), resulting in a higher drying rate and, thus, it is not undesired (Overcashier et al., 1999).

Statistical analysis of the freeze-dried nanosuspensions

When using the additives concentration of the 2^2 design of experiments previously presented (Table 2), it is possible to easily quantify the effect of the various parameters, namely the lyoprotectant concentration (parameter A) and the steric stabilizer concentration (parameter B). Let us define:

- *a* as the combination of parameter A at the high level (5% w/w) and parameter B at the low level (2.5% w/w),
- *b* as the combination of parameter B at the high level (5% w/w) and parameter A at the low level (2.5% w/w),
- *ab* as the combination of parameters A and B at the high level (5% w/w),
- (1) as combination of parameters A and B the low level (2.5% w/w).

Let *n* be the number of repetitions of the test (*n* = 5 in our experimental investigation), and let d_p^j be the mean diameter of the particles for the *j*-th combination of the operating parameters. The effects of the various parameters were then calculated using the approach shown, among the others, by Montgomery (2005). The effect of the parameter A can be calculated considering the following contributions:

- $\left[d_p^a - d_p^{(1)}\right]/n$ in case the value of B is low;

- $\left[d_p^{ab} - d_p^b\right]/n$ in case the value of B is high.

By averaging the single effects calculated previously, the total effect of A on the nanoparticles size is obtained:

$$E(A) = \frac{1}{2n}\left[d_p^a - d_p^{(1)} + d_p^{ab} - d_p^b\right] \quad (1)$$

Similarly, the effect of parameter B can be calculated. Interactions between the two factors can be computed by means of equation (2):

$$E(AB) = \frac{\left[d_p^{ab} - d_p^b - d_p^a + d_p^{(1)}\right]}{2n} \quad (2)$$

Values obtained from equations (1)-(2) can be positive or negative. Positive values mean that when the value of the parameter is increased, then mean particle size increases, and vice versa in case the effect is negative. The analysis of variance "ANOVA" (Montgomery, 2005) was also performed, using the Fisher test, aiming to check the significance of differences between the arithmetic means of the various groups.

Entrapment efficiency

In the test carried out with the drug, with the goal to assess the entrapment efficiency and, thus, that the drug is effectively contained in the polymeric nanoparticles, at first it was necessary to separate the nanoparticles from the liquid medium. Ultracentrifugation (Thermo Scientific SL16, with fixed angle rotor Fiberlite F15-6x100y, 25°, Rmax 98 mm) was used to this purpose. 1 hour at 12000 rpm was sufficient to get a perfect separation of nanoparticles from the liquid medium (supernatant). Ciprofloxacin content in the liquid was measured through UV-spectrofotometry at 270 nm, according to Nijhu et al. (2011) (Cary 60 UV-VIS Spectrophotometer, Agilent, Santa Clara, CA, USA). The entrapment efficiency (%) was

estimated as the difference between the total amount of ciprofloxacin used in the nanoparticle synthesis stage and its amount in the supernatant obtained after the centrifugation step.

Results and discussion

The experimental investigation was initially focused on the comparison of the nanoparticles characteristics in case the CIJM or the MIVM are used. In both cases, acetone was the solvent used for PCL, and the flow rate for each stream was 80 ml min^{-1}; when the MIVM was used for particles synthesis, three different ways of feeding were tested, as summarized in Table 1. With respect to the feeding conditions, it has to be pointed out that the flow rate of the solvent stream, containing the polymer, and that of the aqueous stream containing the chitosan are the same in both reactors, but the hydrodynamics is different: this is due to the fact that the geometry of the two devices is different, and to the fact in the MIVM the total flow rate is double with respect to that of the CIJM. Results are shown in Figure 3. When using the CIJM, the mean particle size was 265±31 nm, with a Zeta potential of 9.8±2.4 mV, while in case the MIVM is used, the mean particle size of the produced nanoparticles was lower, and the Zeta potential higher, thus making these particles more interesting for drug delivery through mucosal route. In particular, the mean particle size was 163±7 nm when using the α feeding way, 204±13 nm when using the β way, and 186±15 nm when using the γ way. It has to be highlighted that the two microreactors are characterized by a different ratio between the solvent and the water stream: in the CIJM, as the quench ratio is 1, the ratio between the solvent and the water flow rate is 0.5, while in the MIVM this ratio is 1/3. In any case, the effect of the dilution was shown to be negligible for values of the quench ration lower than 1 (Zelenková et al., 2017). With respect to the Zeta potential, the value was 31.4±3.7 mV when using the α feeding way, 21.4±3.7 mV when using the β way, and 20.0±4.4 mV when using the γ way. These results evidence that the way in which the various reactants are fed to the

MIVM has a weak influence on the characteristics of the nanoparticles produced in this mixer. This confirms the results by Liu et al. (2008a) for a different system; anyway, slightly better results appear to be obtained in case the α way was used to feed the reactants and, thus, this method was used in the following experiments.

With the goal of investigating the effect of the solvent, nanoparticles were produced, both in the CIJM and in the MIVM, using TBA instead of acetone. Results are shown in Figure 4, where the mean particle size and the Zeta potential obtained in case the solvent is acetone are also shown for comparison. As concerns the CIJM, the use of TBA instead of acetone does not appear advisable. In fact, in this case the mean particle size increased to 942±124 nm, while employing the MIVM, the presence of TBA does not appear to worsen the particle characteristics with respect to those obtained using acetone. In fact, the mean size of the nanoparticles was 221±44 nm and the Zeta potential was 27.1±6.8 mV. Taking into account that the use of TBA allows simplifying the manufacturing process, as the solvent evaporation stage is not required before freeze-drying, further investigation will be focused on the use of this solvent in the synthesis stage.

One of the most important operating parameters of the MIVM is the feeding flow rate. The effect of this parameter on both particle size and Zeta potential has been investigated through experimental investigations, and results are shown in Figure 5. It appears that the feed flow rate has a weak effect on the mean particle diameters in the range 20-80 ml min^{-1}, where a particle diameter of 233±24 nm was obtained at 20 ml min^{-1}, and 221±44 nm was obtained at 80 ml min^{-1}, although a slight increase of the particle diameter was observed at flow rates higher than 100 ml min^{-1} (261±13 nm at 100 ml min^{-1}, 275±18 nm at 120 ml min^{-1}). With respect to the Zeta potential of the nanoparticles, it was almost unaffected by the feed flow rate, taking also into account the variability of this parameter in each experiment (being equal to 25.6±2.7 mV at 20 ml min^{-1}, 26.8±4.6 mV at 120 ml min^{-1}).

The study was continued investigating the stability of the nanoparticles in a long-term period. Figure 6 shows the mean size and the Zeta potential of the chitosan coated PCL nanoparticles as a function of storage time. The suspensions, produced with two different flow rates, namely 20 and 80 ml min^{-1}, were stored at room temperature (around 20°C) for 2 months. From the results shown in Figure 6, it is possible to assess that the size of the nanoparticles does not significantly change with time in all cases.

The second part of the study was devoted to the investigation of the effect of the freeze-drying process on the mean particle size. At first, a standard 2^2 design of experiment was used to assess the effect of sucrose/mannitol with Poloxamer 388/Cremophor EL. Table 2 shows the percentage of the various lyoprotectants/steric stabilizers considered in this study, while Figure 7 shows the mean value of particle diameter obtained in the various cases, and Figure 8 shows the values of the effects calculated using equations (1) and (2).

Let us focus on the sucrose-Cremophor EL couple of additives (Figure 7, graph a; Figure 8, graph a). It appears that when the concentration of both sucrose and Cremophor EL was “low”, i.e. 2.5%, particle diameter increases to a higher value with respect to the case when the concentration of both was “high”, i.e. 5% (378±14 nm vs. 256±11 nm); intermediate results are obtained in case the concentration of one excipient was “low” and that of the other was “high”. When evaluating the effect of the two components, it appears that when the concentration of both sucrose and Cremophor EL is increased, the particle size decreases (the effect is negative), and that sucrose is more effective then Cremophor EL. In case Poloxamer 388 was used with sucrose results are shown in Figure 7 (graph b) and Figure 8 (graph b). In this case it appears that the final mean size of the nanoparticles was not significantly affected by the amount of Poloxamer 388 and of sucrose, being equal to 322±7 nm when their concentration was at the “low value”, and to 313±5 when both concentrations were at the “high” value. These results show that Poloxamer 388 was much more effective than

Cremophor EL in preventing particle aggregation during the freeze-drying process, and that there are no significant advantages in increasing the Poloxamer 388 concentration from 2.5% to 5%: in fact, as the analysis of the effects points out, when considering the mixture of sucrose and Poloxamer 388 the effect of sucrose was negative (the absolute value was lower than that obtained in the couple sucrose-Cremophor EL), but the effect of Poloxamer 388 was (slightly) positive. The conclusion of this study is that Poloxamer 388 has to be preferred as steric stabilizer, when using sucrose, and that 2.5% of sucrose and 2.5% of Poloxamer 388 are the optimal concentrations (resulting in final mean particle size of 306±8 nm).

Beside sucrose, mannitol is another excipient frequently used when freeze-drying pharmaceutical formulations. Results of the study are shown in Figure 7, graphs c and d, and Figure 8, graphs c and d. Let us focus on the mannitol-Cremophor EL couple of additives (Figure 7, graph c; Figure 8, graph c). Results show that when the concentration of both mannitol and Cremophor EL was “low”, i.e. 2.5%, particle diameter increases to a significantly higher value with respect to the case when both concentration was “high”, i.e. 5% (1294±123 nm vs. 853±20 nm). The best result, namely 592±27 nm, was obtained when mannitol concentration was 5%, and Cremophor EL concentration was 2.5%. When evaluating the effect of the two components, it appears that when the concentration of both mannitol and Cremophor EL is increased, the particle size decreases (the effect is negative), and increasing mannitol concentration is more effective then increasing the concentration of Cremophor EL. Increasing both concentrations should be avoided as the effect was positive, i.e. the mean particle size increased. In case Poloxamer 388 is used with mannitol results are shown in Figure 7 (graph d) and Figure 8 (graph d). In this case, it appears that when the concentration of both mannitol and Poloxamer 388 was “low”, i.e. 2.5%, particle diameter increased to a higher value with respect to the case when both concentration was “high”, i.e. 5% (470±13 nm vs. 380±10 nm); intermediate results were obtained in case the concentration

of one excipient was “low” and that of the other was “high”. When evaluating the effect of the two components, it appears that when the concentration of both mannitol and Poloxamer 388 was increased, the particle size decreased (the effect is negative), and that mannitol was more effective then Poloxamer 388. These results show that Poloxamer 388 is much more effective than Cremophor EL in preventing particle aggregation during the freeze-drying process, also in case mannitol is used as excipient, and that the optimal excipient composition for this formulation is mannitol 5% and Poloxamer 5%. Nevertheless, the best result was obtained with the 2.5% sucrose - 2.5% Poloxamer 388 mixture.

In the previous study, the total solute concentration in the formulations being freeze-dried was not constant, as it ranged from 5 to 10%. Thus, the study of the effect of Cremophor EL and of Poloxamer, in presence of sucrose or of mannitol was repeated using the values shown in Table 3, i.e. with a total solute concentration of 5%. Figure 9, graphs a and c, shows the results obtained when using sucrose, alone, or with Cremophor EL or with Poloxamer 388. Sucrose alone was not particularly effective, as the final mean size of the nanoparticles was 567±109 nm. Better results were obtained when using Cremophor EL with sucrose, because the mean particle size after the freeze-drying process decreased from 494±45 nm to 382±40 nm when Cremophor EL concentration was increased from 1% to 2.5% (and the sucrose concentration is decreased from 4% to 2.5%). Even better results were obtained in presence of Poloxamer 388, and also in those experiments the results were almost unaffected by the percentage of Poloxamer 388, being the mean diameter equal to 325±9 nm with 1% of Poloxamer 388 (and 4% of sucrose), and to 322±11 nm with 2.5% of Poloxamer 388 (and 2.5% of sucrose). With respect to the Zeta potential, it remained positive in all case, with values higher than +30 mV. When mannitol was used as excipient, results were significantly worsened, as it appears from Figure 9, graph b. The mean particle size increased up to 1368±130 nm when only mannitol was present in the system, while slightly better results

were obtained in presence of Cremophor EL (698±69 nm with 4% mannitol and 1% Cremophor EL). Better results were obtained in presence of Poloxamer 388, 456±15 nm when Poloxamer concentration was 1% (and mannitol is 4%) and 457±29 nm when Poloxamer concentration was 2.5% (and mannitol is 2.5%). In all cases, the couple sucrose-Poloxamer 388 appears to be the optimal one for particle stabilization in the freeze-drying process, and the nanoparticles obtained appear to be perfectly suitable for the desired delivery through the mucosal route.

As it was stated in the Introduction, the investigation was carried out in absence of a drug, aiming to focus on the manufacturing system, as quite often the presence of the drug does not affect significantly the final mean particle size, especially when it is entrapped in the polymeric matrix. The optimization of the drug encapsulation in the optimal manufacturing system identified in this work will be the subject of a future paper, but some preliminary tests have been carried out with ciprofloxacin, to test that (i) the drug is effectively entrapped in the particles, and that (ii) the presence of this drug, entrapped in the polymeric nanoparticles, poorly affects the particles size and the zeta potential. Experiments was carried out in the MIVM, using TBA as polymer solvent. Results are shown in Figure 10: graphs a and b show the comparison between the values of mean particles diameter and zeta potential, respectively, with or without the drug, while graph c shows the values of mean particles diameter obtained for different ciprofloxacin concentrations in the feed. Results point out that the presence of this drug has a poor effect on the investigated parameters. The measured drug entrapment efficiency was 61.2%.

Conclusions

The manufacturing of chitosan coated PCL nanoparticles using the solvent displacement method in two different microreactors, namely the confined impinging jets mixer and the

multi inlet vortex mixer, was investigated in this paper, considering also the following freeze-drying stage, aiming to provide long term stability to the nanoparticles. Results evidenced that the MIVM can be used as an alternative to the CIJM, as it allows avoiding the quenching. In case TBA is used as PCL solvent, the nanosuspension can be directly freeze-dried and, thus, the solvent evaporation stage is no longer necessary. Suitable lyoprotectants and steric stabilizers have to be added to the formulation. Nanoparticles with a mean diameter of 221±44 nm were obtained in the MIVM, with a Zeta potential of 27.1±6.8 mV, thus perfectly suitable to fulfill the mucoadhesive function. The optimal combination of excipients for the freeze-drying stage resulted to be 5% sucrose/2.5% Poloxamer 388, being the final size of the nanoparticles of 306±8 nm with a Zeta potential larger than +30 mV. Future investigations will focus on the encapsulation of a test drug, ciprofloxacin, in the nanoparticles produced through this way, and on the study of the release of this drug.

Acknowledgement

Financial support of the Bilateral Cooperation Project between Italy and Argentina (AR14MO8) is gratefully acknowledged. The authors would like to thank Eleonora Barbirato for the contribution to the experimental investigation.

List of symbols

c_{chi}	chitosan concentration, mg ml^{-1}
c_p	polymer concentration, mg ml^{-1}
$c_{pol\ 388}$	Poloxamer 388 concentration, mg ml^{-1}
d_p	particle diameter, nm
E	effect
M_w	molecular weight, kg kmol^{-1}
n	number of repetitions of each test
$p_{chamber}$	chamber pressure, Pa
T_{shelf}	temperature of the heating shelf, K

Abbreviations

CIJM	Confined Impinging Jets Mixer
FR	Flow rate, ml min^{-1}
MIVM	Multi Inlet Vortex Mixer
PCL	Polycaprolactone
W/A	Water to Acetone ratio

List of references

Abdelwahed, W., Degobert, G., Fessi, H., 2006a. Investigation of nanocapsules stabilization by amorphous excipients during freeze-drying and storage. Eur. J. Pharm. Biopharm. 63, 87–94. https://doi.org/10.1016/j.ejpb.2006.01.015

Abdelwahed, W., Degobert, G., Fessi, H., 2006b. Freeze-drying of nanocapsules: Impact of annealing on the drying process. Int. J. Pharm. 324, 74–82. https://doi.org/10.1016/j.ijpharm.2006.06.047

Abdelwahed, W., Degobert, G., Stainmesse, S., Fessi, H., 2006c. Freeze-drying of nanoparticles: Formulation, process and storage considerations. Adv. Drug Deliv. Rev. 58, 1688–1713. https://doi.org/10.1016/j.addr.2006.09.017

Andrews, G.P., Laverty, T.P., Jones, D.S., 2009. Mucoadhesive polymeric platforms for controlled drug delivery. Eur. J. Pharm. Biopharm. 71, 505–518. https://doi.org/10.1016/j.ejpb.2008.09.028

Barresi, A.A., Vanni, M., Fissore, D., Zelenková, T., 2015. Synthesis and preservation of polymer nanoparticles for pharmaceuticals applications, in: Thakur., V.K., Thakur, M.K. (Eds.), Handbook of Polymers for Pharmaceutical Technologies: Processing and Applications, Volume 2, John Wiley & Sons, Inc., Hoboken, pp. 229-280.

Beirowski, J., Inghelbrecht, S., Arien, A., Gieseler, H., 2011a. Freeze drying of nanosuspensions, 1: Freezing rate versus formulation design as critical factors to preserve the original particle size distribution. J. Pharm. Sci. 100, 958–1968. https://doi.org/10.1002/jps.22425

Beirowski, J., Inghelbrecht, S., Arien, A., Gieseler, H., 2011b. Freeze drying of nanosuspensions, 2: The role of the critical formulation temperature on stability of drug nanosuspensions and its practical implication on process design. J. Pharm. Sci. 100,

4471–4481. https://doi.org/ 10.1002/jps.22634

Beirowski, J., Inghelbrecht, S., Arien, A., Gieseler, H., 2011c. Freeze drying of nanosuspensions, Part 3: Investigation of factors compromising storage stability of highly concentrated drug nanosuspensions. J. Pharm. Sci. 101, 354-362. https://doi.org/10.1002/jps.22745

Bordes, C., Fréville, V., Ruffin, E., Marote, P., Gauvrit, J.Y., Briançon, S., Lantéri, P. 2010. Determination of poly(ε-caprolactone) solubility parameters: Application to solvent substitution in a microencapsulation process. Int. J. Pharm. 383, 236-243. https://doi.org/10.1016/j.ijpharm.2009.09.023

Blondeau, J. M., 2004. Fluoroquinolones: mechanism of action, classification, and development of resistance. Sur. Ophthalm. 49, S73–S78. https://doii.org/10.1016/j.survophthal.2004.01.005.

Chawla, J. S., Amiji, M.M., 2002. Biodegradable poly(ε-caprolactone) nanoparticles for tumor-targeted delivery of tamoxifen. Int. J. Pharm. 249, 127–138. https://doi.org/10.1016/S0378-5173(02)00483-0

Chowdary, K.P., Rao, Y.S., 2004. Mucoadhesive microspheres for controlled drug delivery. Biol. Pharm. Bull. 27, 1717-1724.

Crowe, J.H., Crowe, L.M., Carpenter, J.F., 1993. Preserving dry biomaterials: The water replacement hypothesis. Biopharm. 6, 28–37.

Dash, M., Chiellini, F., Ottenbrite, R.M., Chiellini, E., 2011. Chitosan - A versatile semi-synthetic polymer in biomedical applications. Progr. Pol. Sci. 36, 981–1014. https://doi.org/10.1016/j.progpolymsci.2011.02.001

DeAssis, D.N., Mosqueira, V.C., Vilela, J.M., Andrade, M.S., Cardoso, V.N., 2008. Release profiles and morphological characterization by atomic force microscopy and photon correlation spectroscopy of ^{99m}Technetium—fluconazole nanocapsules. Int. J. Pharm.

349, 152–60. https://doi.org/10.1016/j.ijpharm.2007.08.002

Di Pasquale, N., Marchisio, D.L., Barresi, A.A., 2012. Model validation for precipitation in solvent-displacement processes. Chem. Eng. Sci. 84, 671-683. https://doi.org/10.1016/j.ces.2012.08.043

Dumortier, G., Grossiord, J.L., Agnely, F., Chaumeil, J.C., 2006. A review of Poloxamer 407 pharmaceutical and pharmacological characteristics. Pharm. Res. 23, 2709–2728. https://doi.org/ 10.1007/s11095-006-9104-4

Fessi, H., Puisieux, J.P., Devissaget, N., Ammoury, N., Benita, S., 1989. Nanocapsule formation by interfacial polymer deposition following solvent displacement. Int. J. Pharm. 55, R1–R4. https://doi.org/10.1016/0378-5173(89)90281-0

Gavi, E., Rivautella, L., Marchisio, D.L., Vanni, M., Barresi, A.A., Baldi, G., 2007. CFD modelling of nano-particle precipitation in confined impinging jet reactors. Chem. Eng. Res. Des. 85, 735-744. https://doi.org/10.1205/cherd06176

Gelderblom, H., Verweij, J., Nooter, K., Sparreboom, A., 2001. Cremophor EL: The drawbacks and advantages of vehicle selection for drug formulation. Eur. J. Cancer 37, 1590–1598.

Gupta, N.K., Tomar, P., Sharma, V., Dixit, V.K., 2011. Development and characterization of chitosan coated poly-(ε-caprolactone) nanoparticulate system for effective immunization against influenza. Vaccine, 29, 9026-9037. https://doi.org/10.1016/j.vaccine.2011.09.033

He, Z., Santos, J.L, Tian, H., Huang, H., Hu, Y., Liu, L., Leong, K.W., Chen, Y., Mao, H.Q., 2017. Scalable fabrication of size-controlled chitosan nanoparticles for oral delivery of insulin. Biomaterials, 130, 28-41. https://doi.org/10.1016/j.biomaterials.2017.03.028

Hickey, J.W., Santos, J.L., Williford, J.M., Mao, H.Q., 2015. Control of polymeric nanoparticle size to improve therapeutic delivery. J. Contr. Release 219, 536-547.

https://doi.org/10.1016/j.jconrel.2015.10.006

Horn, D., Rieger, J., 2001. Organic nanoparticles in the aqueous phase - theory, experiment, and use. Angewandte Chem. Int. Ed. 40, 4330-4361. https://doi.org/ 10.1002/1521-3773(20011203)40:23<4330::AID-ANIE4330>3.0.CO;2-W

Huang, Y., Leobandung, W., Foss, A., Peppas, N.A., 2000. Molecular aspects of muco- and bioadhesion: Tethered structures and site-specific surfaces. J. Contr. Release, 65, 63-71. https://doi.org/10.1016/S0168-3659(99)00233-3

Issa, M., Koping-Hoggard, M., Artursson, P., 2005. Chitosan and the mucosal delivery of biotechnology drugs. Drug Discov. Today Technol. 2, 1–6. https://doi.org/10.1016/j.ddtec.2005.05.008

Johnson, B.K., Prud'homme, R.K., 2003a. Flash nanoprecipitation of organic actives and block copolymers using a Confined Impinging Jets Mixers. Austral. J. Chem. 56, 1021–1024. https://doi.org/10.1071/CH03115

Johnson, B. K., Prud'homme, R.K., 2003b. Mechanism for rapid self-assembly of block copolymer nanoparticles. Phys. Rev. Lett. 91, 118302-118305. https://doi.org/ 10.1103/PhysRevLett.91.118302

Jores, K., Mehnert, W., Drecusler, M., Bunyes, H., Johan, C., Mader, K., 2004. Investigations on the structure of solid lipid nanoparticles (SLN) and oil-loaded solid lipid nanoparticles by photon correlation spectroscopy, field-flow fractionation and transmission electron microscopy. J. Cont. Rel. 95, 217–227. https://doi.org/ 10.1016/j.jconrel.2003.11.012

Kasraian, K., DeLuca, P.P., 1995. Thermal analysis of the tertiary butyl alcohol-water system and its implications on freeze-drying. Pharm. Res. 12, 484–490. https://doi.org/10.1023/A:1016233408831

Lee, K.Y., Ha, S.W., Park, W.H., 1995. Blood biocompatibility and biodegradability of

partially N-acylated chitosan derivatives. Biomaterials, 16,1211–1216. https://doi.org/10.1016/0142-9612(95)98126-Y

Lehr, C.M., Bouwstra, J.A., Schacht, E.H., Junginger, H.E., 1992. In vitro evaluation of mucoadhesive properties of chitosan and some other natural polymers. Int. J. Pharm. 78, 43–48. https://doi.org/10.1016/0378-5173(92)90353-4

Lince, F., Marchisio, D.L, Barresi, A.A., 2008. Strategies to control the particle size distribution of poly-ε-caprolactone nanoparticles for pharmaceutical applications. J. Colloid Interface Sci. 322, 505–515. https://doi.org/10.1016/j.jcis.2008.03.033

Lince, F., Marchisio, D.L., Barresi, A.A., 2009. Smart mixers and reactors for the production of pharmaceutical nanoparticles: Proof of concept. Chem. Eng. Res. Des. 87, 543–549. https://doi.org/10.1016/j.cherd.2008.11.009

Lince, F., Bolognesi, S., Stella, B., Marchisio, D.L., Dosio, F., 2011a. Preparation of polymer nanoparticles loaded with doxorubicin for controlled drug delivery. Chem. Eng. Res. Des. 89, 2410–2419. https://doi.org/10.1016/j.cherd.2011.03.010

Lince, F., Bolognesi, S., Marchisio, D.L., Stella, B., Dosio, F., Barresi, A.A., Cattel, L., 2011b. Preparation of poly(MePEGCA-co-HDCA) nanoparticles with confined impinging jets reactor: Experimental and modeling study. J. Pharm. Sci. 100, 2391–2405. https://doi.org/10.1002/jps.22451

Lince, F., Marchisio, D.L., Barresi, A.A., 2011c. A comparative study for nanoparticle production with passive mixers via solvent-displacement: Use of CFD models for optimization and design. Chem. Eng. Proc. 50, 356-368. https://doi.org/10.1016/j.cep.2011.02.015

Liu, Y., Cheng, C., Liu, Y., Prud'homme, R.K., Fox, R.O., 2008a. Mixing in a multi-inlet vortex mixer (MIVM) for flash nano-precipitation. Chem. Eng. Sci. 63, 2829–2842. https://doi.org/10.1016/j.ces.2007.10.020

Liu, Y., Tong, Z., Prud'homme, R.K., 2008b. Stabilized polymeric nanoparticles for controlled and efficient release of bifenthrin. Pest Manag. Sci. 64, 808–812. https://doi.org/10.1002/ps.1566

Marchisio, D.L., Rivautella, L., Barresi, A.A., 2006. Design and scale-up of chemical reactors for nanoparticle precipitation. AIChE J. 52, 1877-1887. https://doi.org/ 10.1002/aic.10786

Marchisio, D.L., Omegna, F., Barresi, A.A., Bowen, P. 2008. Effect of mixing and other operating parameters in sol-gel processes. Ind. Eng. Chem. Res. 47, 7202–7210. https://doi.org/ 10.1021/ie800217b

Marchisio, D.L., Omegna, F., Barresi, A.A., 2009. Production of TiO_2 nanoparticles with controlled characteristics by means of a Vortex Reactor. Chem. Eng. J. 146, 456–465. https://doi.org/10.1016/j.cej.2008.10.031

Mazzarino, L., Travelet, C., Ortega-Murillo, S., Otsuka, I., Pignot-Paintrand, I., Lemos-Senna, E., Borsali, R., 2012. Elaboration of chitosan-coated nanoparticles loaded with curcumin for mucoadhesive applications. J. Colloid Interface Sci. 370, 58-66. https://doi.org/10.1016/j.jcis.2011.12.063

Merisco-Liversidge, E., Liversidge, G.G., Cooper, E.R., 2003. Nanosizing: A formulation approach for poorly-water-soluble compounds. Eur. J. Pharm. Sci. 18, 113–120. https://doi.org/10.1016/S0928-0987(02)00251-8

Mersmann, A., 1999. Crystallization and precipitation: The optimal supersaturation. Chem. Eng. Proc. 71, 1240–1244. https://doi.org/10.1002/cite.33071110

Montgomery, D.C., 2005. Design and Analysis of Experiments, 6th ed. John Wiley & Sons Inc, New York.

Nagavarma, B.V.N., Hemant, K.S.Y., Ayaz, A., Vasudha, L.S., Shivakumar, H.G., 2012. Different techniques for preparation of polymeric nanoparticles–A review. Asian J.

Pharm. Clin. Res. 5, 16–23.

Ni, N., Tesconi, M., Tabibi, S.E., Gupta, S., Yalkowsky, S. H., 2001. Use of pure *t*-butanol as a solvent for freeze-drying: A case study. Int. J. Pharm. 226, 39–46. https://doi.org/10.1016/S0378-5173(01)00757-8

Nijhu, R.S., Jhanker, Y.M., Sutradhar, K.B., 2011. Development of an assay method for simultaneous determination of ciprofloxacin and naproxen by UV spectrophotometric method. Stamford J. Pharm. Sci. 4, 84-90.

Nishimura, K., Ishihara, C., Ukei, S., Tokura, S., Azuma, I., 1986. Stimulation of cytokine production in mice using deacetylated chitin. Vaccine 4, 151–156. https://doi.org/10.1016/0264-410X(86)90002-2

Overcashier, D.E., Patapoff , T.W., Hsu, C.C., 1999. Lyophilization of protein formulations in vials: Investigation of the relationship between resistance to vapor flow during primary drying and small-scale product collapse. J. Pharm. Sci. 99, 688-695. https://doi.org/10.1021/js980445+

Otsuka, H., Beletsi, A., Nagasaki, Y., Kataoka, K., 2003. PEG-ylated nanoparticles for biological and pharmaceutical application. Adv. Drug. Del. Rev. 24, 403–419. https://doi.org/10.1016/S0169-409X(02)00226-0

Peracchia, M.T., Vauthier, C., Desmaele, D., Gulik, A., Dedieu, J.C., Demoy, M., d'Angelo, J., Couvreur, P., 1998. Pegylated nanoparticles from a novel methoxypolyethylene glycol cyanoacrylate hexadecyl cyanoacrylate amphiphilic copolymer. Pharm. Res. 15, 550–556. https://doi.org/10.1023/A:1011973625803

Pikal, M.J., 1999. Mechanisms of protein stabilization during freeze-drying and storage. The relative importance of thermodynamic stabilization and glassy state relaxation dynamics. Drugs Pharm. Sci. 96, 161–198.

Pisano R., Fissore D., Barresi A. A., 2014. Intensification of freeze-drying for the

pharmaceutical and food industries. n: Modern Drying Technology - Volume 5: Process Intensification (Tsotsas E., Mujumdar A. S., editors), 131-162, Wiley-VCH Verlag GmbH & Co. KGaA, Weinheim. https://doi.org/10.1002/9783527631704.ch05

Rampino, A., Borgogna, M., Blasi, P., Bellich, B., Cesàroa, A., 2013. Chitosan nanoparticles: Preparation, size evolution and stability. Int. J. Pharm. 455, 219– 228. https://doi.org/10.1016/j.ijpharm.2013.07.034

Shen, H., Hong, S., Prud'homme, R.K., Liu, Y., 2011. Self-assembling process of flash nanoprecipitation in a multi-inlet vortex mixer to produce drug-loaded polymeric nanoparticles. J. Nanopart. Res. 13, 4109–4120. https://doi.org/10.1007/s11051-011-0354-7

Teagarden, D.L., Baker, D.S., 2001. Practical aspects of lyophilization using non-aqueous co-solvent systems. Eur. J. Pharm. Sci. 15, 115–133. https://doi.org/10.1016/S0928-0987(01)00221-4

Valente, I., Celasco, E., Marchisio, D. L., Barresi, A. A., 2012. Nanoprecipitation in confined impinging jets mixers: Production, characterization and scale-up of pegylated nanospheres and nanocapsules for pharmaceutical use. Chem. Eng. Sci. 77, 217-277. https://doi.org/ 10.1016/j.ces.2012.02.050

Wilhelmus, K.R., Hyndiuk, R.A., Caldwell, D.R., Abshire, R.L., Folkens, A.T., Godio, L.B., 1993. 0.3% ciprofloxacin ophthalmic ointment in the treatment of bacterial keratitis. The Ciprofloxacin Ointment/Bacterial Keratitis Study Group. Archiv Ophthalmol. 11, 1210–1218.

Wittaya-Areekul, S., Nail, S.L., 1998. Freeze-drying of *tert*-butyl alcohol/water cosolvent systems: Effects of formulation and process variables on residual solvents. J. Pharm. Sci. 87, 491–495. https://doi.org/10.1021/js9702832

Wu, C., Jim, T.F., Gan, Z., Zhao, Y., Wang, S., 2000. A heterogeneous catalytic kinetics for

enzymatic biodegradation of poly(ε-caprolactone) nanoparticles in aqueous solution. Polymer 41, 3593–3597. https://doi.org/10.1016/S0032-3861(99)00586-8

Zelenková, T., Fissore, D., Marchisio, D.L., Barresi, A.A., 2014. Size control in production and freeze-drying of poly-ε-caprolactone nanoparticles. J. Pharm. Sci. 103, 1839-1850. https://doi.org/10.1002/jps.23960

Zelenková, T., Barresi, A.A., Fissore, D., 2015. On the use of tert-butanol/water co-solvent systems in production and freeze-drying of poly-ε-caprolactone nanoparticles. J. Pharm. Sci. 104, 178-190. https://doi.org/10.1002/jps.24271

Zelenková, T., Mora, M.J., Barresi, A.A., Granero, G.E., Fissore, D., 2018. On the production of chitosan coated PCL nanoparticles in a Confined Impinging Jets Reactor. J. Pharm. Sci. *In press*. https://doi.org/ 10.1016/j.xphs.2017.11.020

List of Tables

Table 1. Feeding characteristics in the experiments with the MIVM.

Table 2. Excipients concentration in the freeze-drying study using the 2^2 design of experiments.

Table 3. Excipients concentration in the freeze-drying study carried out with the same value of solute concentration.

List of Figures

Figure 1. Experimental apparatus used for the nanoparticle synthesis by the solvent displacement method in the CIJM (A) and in the MIVM (B) (the infusion pumps and the mixer are evidenced in the picture) and sketch of the mixers.

Figure 2. Experimental measurement of product temperature in two vials of the batch during a freeze-drying cycle with a formulation containing 5% sucrose.

Figure 3. Effect of the feeding configuration on the mean size (graph a) and on the Zeta potential (graph b) for nanoparticles produced in the MIVM using acetone as solvent; results obtained in the CIJM are also shown for comparison (operating conditions: FR = 80 ml min^{-1}, c_p = 5 mg ml^{-1}, $c_{pol\ 388}$ = 2.5 mg ml^{-1}, c_{chi} = 2.5 mg ml^{-1}; for CIJM W/A = 1 and quench volumetric ratio = 1).

Figure 4. Comparison of the mean size (graph (a)) and the Zeta potential (graph (b)) of nanoparticles produced using acetone (■) or TBA (▩) in the CIJM or in the MIVM (operating conditions: FR = 80 ml min^{-1}, c_p = 5 mg ml^{-1}, $c_{pol\ 388}$ = 2.5 mg ml^{-1}, c_{chi} = 2.5 mg ml^{-1}; for CIJM W/A = 1 and quench volumetric ratio = 1; for MIVM feeding configuration α)

Figure 5. Influence of the liquid flow rate on the mean particle size (graph a) and on the Zeta potential (graph b) of nanoparticles composed of PCL (c_p = 5 mg ml^{-1}), Poloxamer 388 ($c_{pol\ 388}$ = 2.5 mg ml^{-1}) and chitosan (c_{chi} = 2.5 mg ml^{-1}) produced in the MIVM using TBA as solvent.

Figure 6. Dependence of the mean size (graph a) and of the Zeta potential (graph b) on time for nanoparticles composed of PCL (c_p = 5 mg ml^{-1}), Poloxamer 388 ($c_{pol\ 388}$ = 2.5 mg ml^{-1}) and chitosan (c_{chi} = 2.5 mg ml^{-1}) produced in the MIVM using TBA as solvent and two different flow rates (■: *FR* = 20 ml min^{-1}, ▲: *FR* = 80 ml min^{-1}).

Figure 7. Comparison of the mean size of the chitosan containing nanoparticles obtained from different water/TBA nanosuspensions (listed in Table 2) before (■) and after (□) freeze–drying (operating conditions: *FR* = 80 ml min^{-1}, c_p = 5 mg ml^{-1}, $c_{pol\ 388}$ = 2.5 mg ml^{-1}, c_{chi} = 2.5 mg ml^{-1}, $p_{chamber}$ = 10 Pa, and T_{shelf} = −20ºC).

Figure 8. Effect of single factors (lyoprotectant (A), steric stabilizer (B)) and of their combination on the size of nanoparticles, obtained from different water/TBA nanosuspensions, after freeze-drying process in case formulations are stabilized with Cremophor EL and sucrose (a), with Poloxamer 388 and sucrose (b), with Cremophor EL and mannitol (c), with Poloxamer 388 and mannitol (d) (operating conditions: *FR* = 80 ml min^{-1}, c_p = 5 mg ml^{-1}, $c_{pol\ 388}$ = 2.5 mg ml^{-1}, c_{chi} = 2.5 mg ml^{-1}, $p_{chamber}$ = 10 Pa, and T_{shelf} = −20ºC).

Figure 9. Comparison of the mean size (graphs a and b) and Zeta potential (graphs c and d) of the chitosan containing nanoparticles obtained from different water/TBA nanosuspensions (listed in Table 3) before (■) and after (□) freeze–drying (operating conditions: *FR* = 80 ml min^{-1}, c_p = 5 mg ml^{-1}, c_{pol388} = 2.5 mg ml^{-1}, c_{chi} = 2.5 mg ml^{-1}, $p_{chamber}$ = 10 Pa, and T_{shelf} = −20ºC).

Figure 10. Comparison of the mean size (graph a) and Zeta potential (graph b) of the nanoparticles without ciprofloxacin (#1) and with the drug (#2, c_{CPX} = 2.5 mg ml^{-1}) obtained

in the MIVM using TBA as polymer solvent. Influence of the ciprofloxacin content on the mean particle size of nanoparticles obtained in the MIVM using TBA al polymer solvent (graph c). In all tests the following operating conditions were used: FR = 80 ml min^{-1}, c_p = 5 mg ml^{-1}, $c_{pol\ 388}$ = 2.5 mg ml^{-1}, c_{chi} = 2.5 mg ml^{-1}.

Table 1

		Feeding configurations		
		α	**β**	**γ**
Stream ID	**1**	Acetone + PCL	Acetone + PCL	Acetone + PCL
	2	Water + Poloxamer 388	Water	Water + Poloxamer 388
	3	Water + chitosan + acetic acid	Water + Poloxamer 388	Water
	4	Water	Water + chitosan + acetic acid	Water + chitosan + acetic acid

Table 2

Sample ID	***Sucrose, %***	***Mannitol, %***	***Cremophor EL, %***	***Poloxamer 388, %***
1	2.5	-	2.5	-
2	5	-	2.5	-
3	2.5	-	5	-
4	5	-	5	-
5	2.5	-	-	2.5
6	5	-	-	2.5
7	2.5	-	-	5
8	5	-	-	5
9	-	2.5	2.5	-
10	-	5	2.5	-
11	-	2.5	5	-
12	-	5	5	-
13	-	2.5	-	2.5
14	-	5	-	2.5
15	-	2.5	-	5
16	-	5	-	5

Table 3

Sample ID	***Sucrose, %***	***Mannitol, %***	***Cremophor EL, %***	***Poloxamer 388, %***
1a	5	-	-	-
2a	4	-	1	-
3a	2.5	-	2.5	-
4a	4	-	-	1
5a	2.5	-	-	2.5
1b	-	5	-	-
2b	-	4	1	-
3b	-	2.5	2.5	-
4b	-	4	-	1
5b	-	2.5	-	2.5

Figure 1

(A)

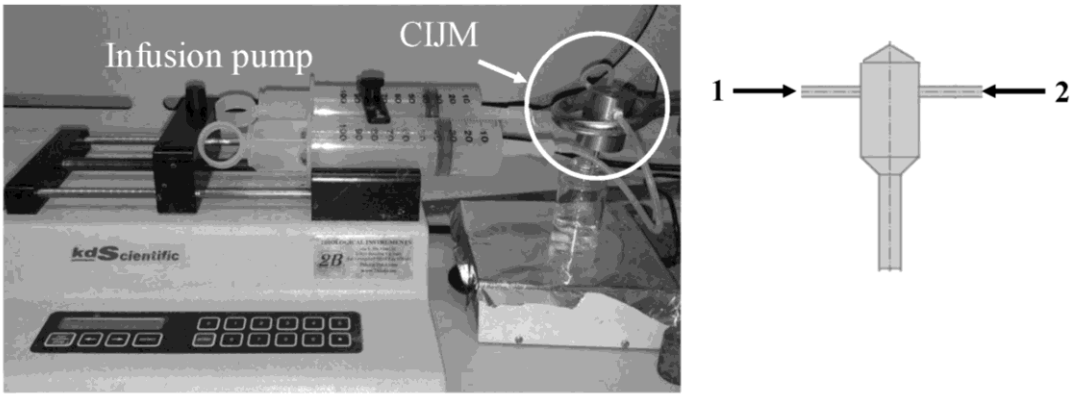
Infusion pump
CIJM
kdScientific
1
2

(B)

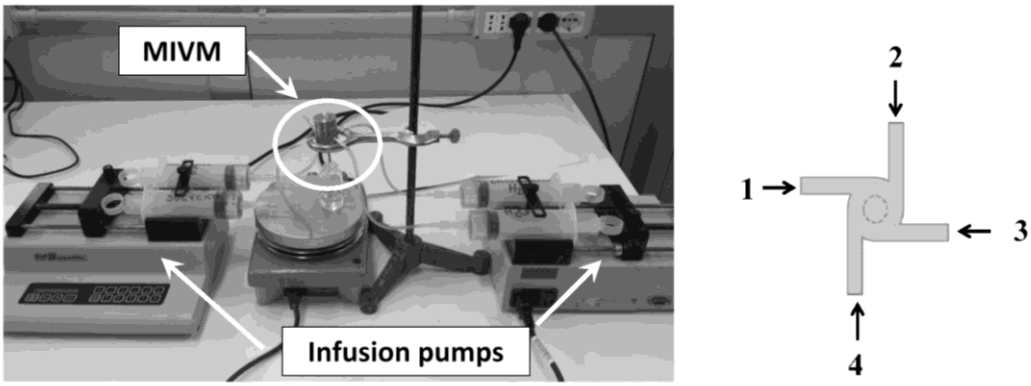
MIVM
Infusion pumps
1
2
3
4

Figure 2

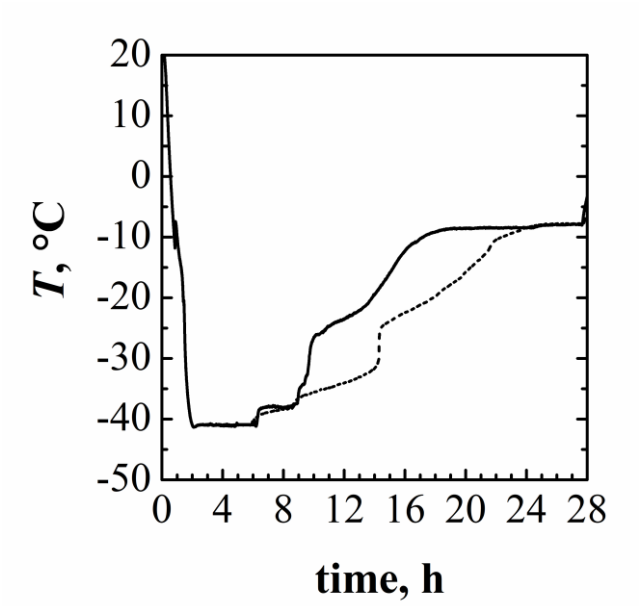

Figure 3

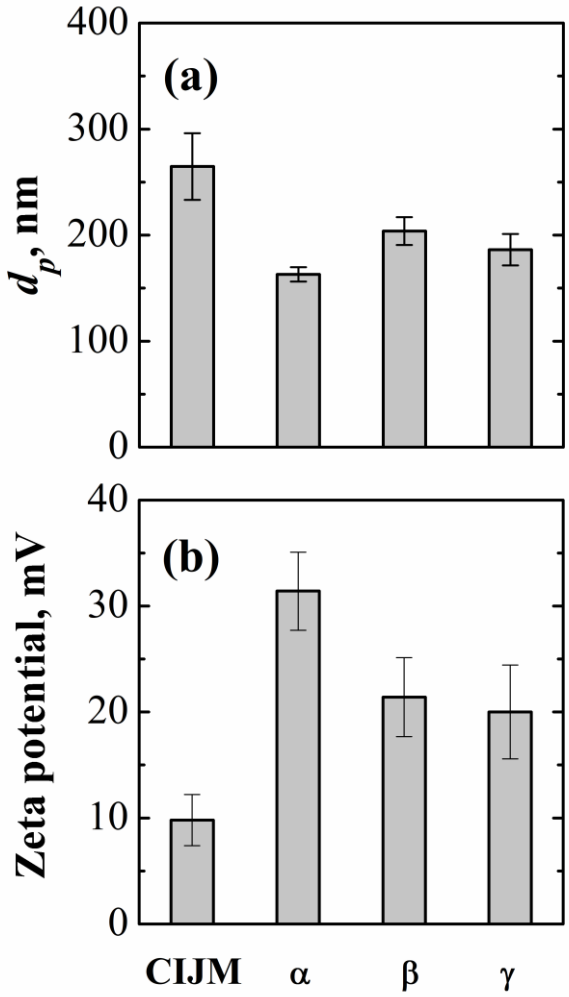
(a)
d_p, nm
400
300
200
100
0
(b)
Zeta potential, mV
40
30
20
10
0
CIJM
α
β
γ

Figure 4

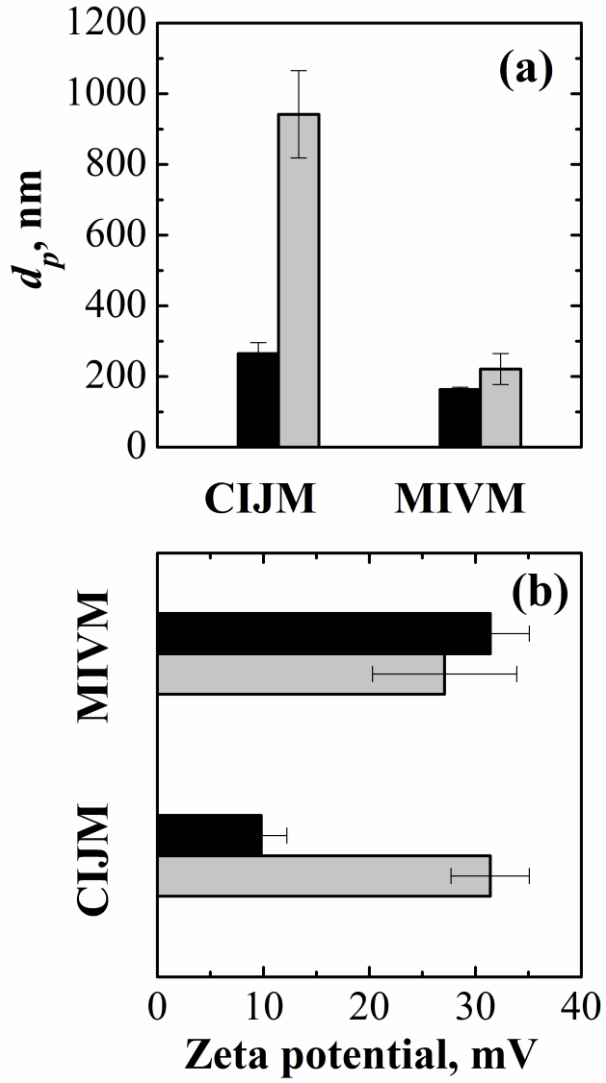
(a)
d_p, nm
1200
1000
800
600
400
200
0
CIJM
MIVM
(b)
MIVM
CIJM
0
10
20
30
40
Zeta potential, mV

Figure 5

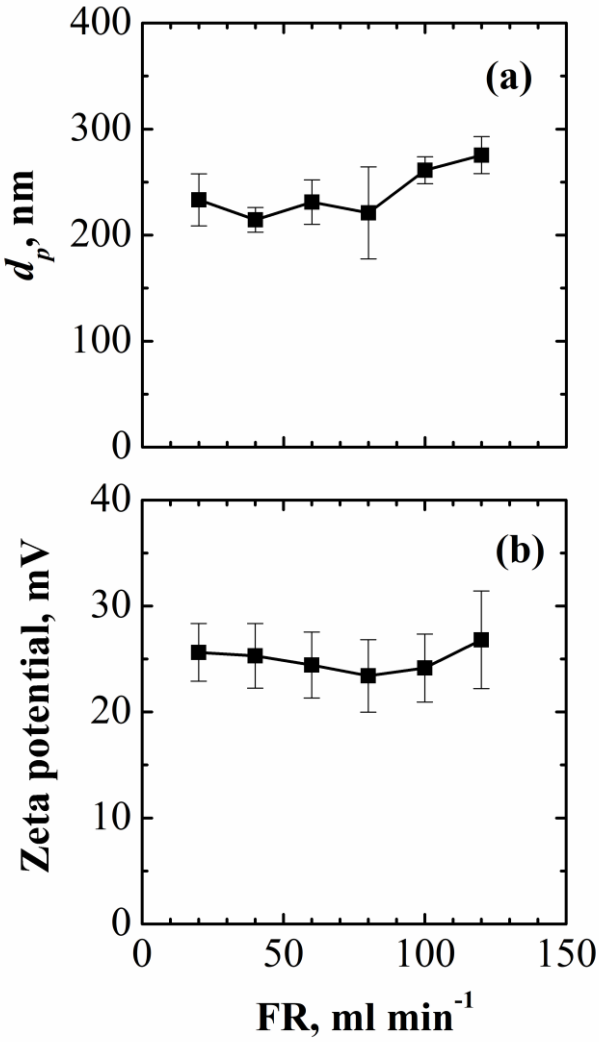
400
300
200
100
0
(a)
d_p, nm
40
30
20
10
0
(b)
Zeta potential, mV
0
50
100
150
FR, ml min^{-1}

Figure 6

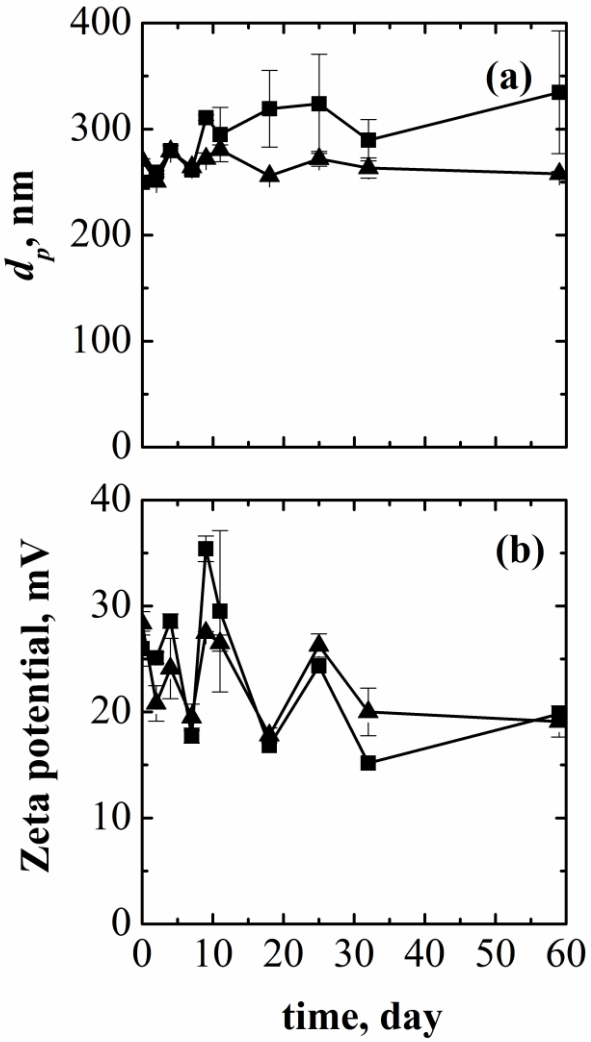
400
300
200
100
0
(a)
d_p, nm
40
30
20
10
0
(b)
Zeta potential, mV
0
10
20
30
40
50
60
time, day

Figure 7

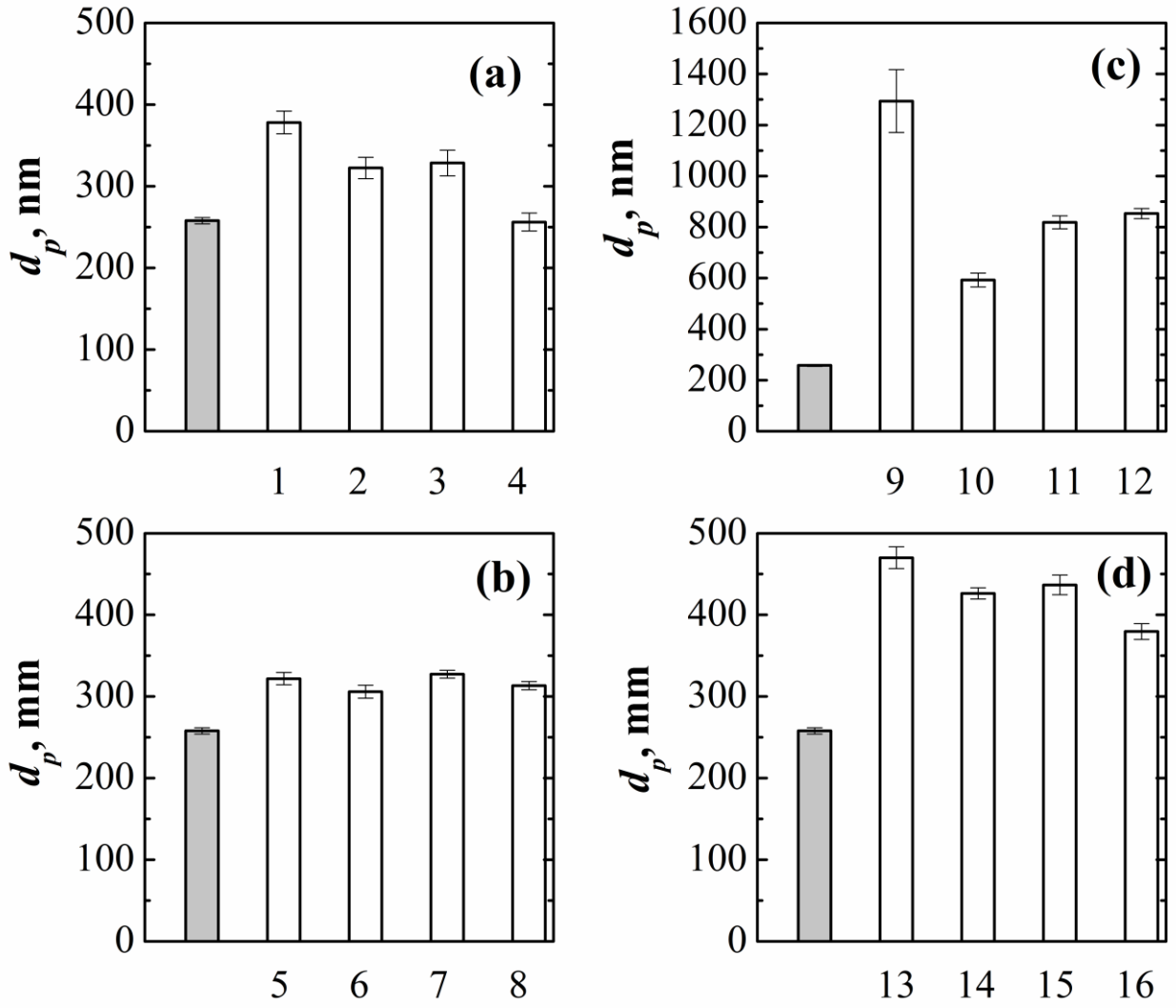
(a)
(b)
(c)
(d)
d_p, nm
d_p, mm
0
100
200
300
400
500
600
800
1000
1200
1400
1600
1
2
3
4
5
6
7
8
9
10
11
12
13
14
15
16

Figure 8

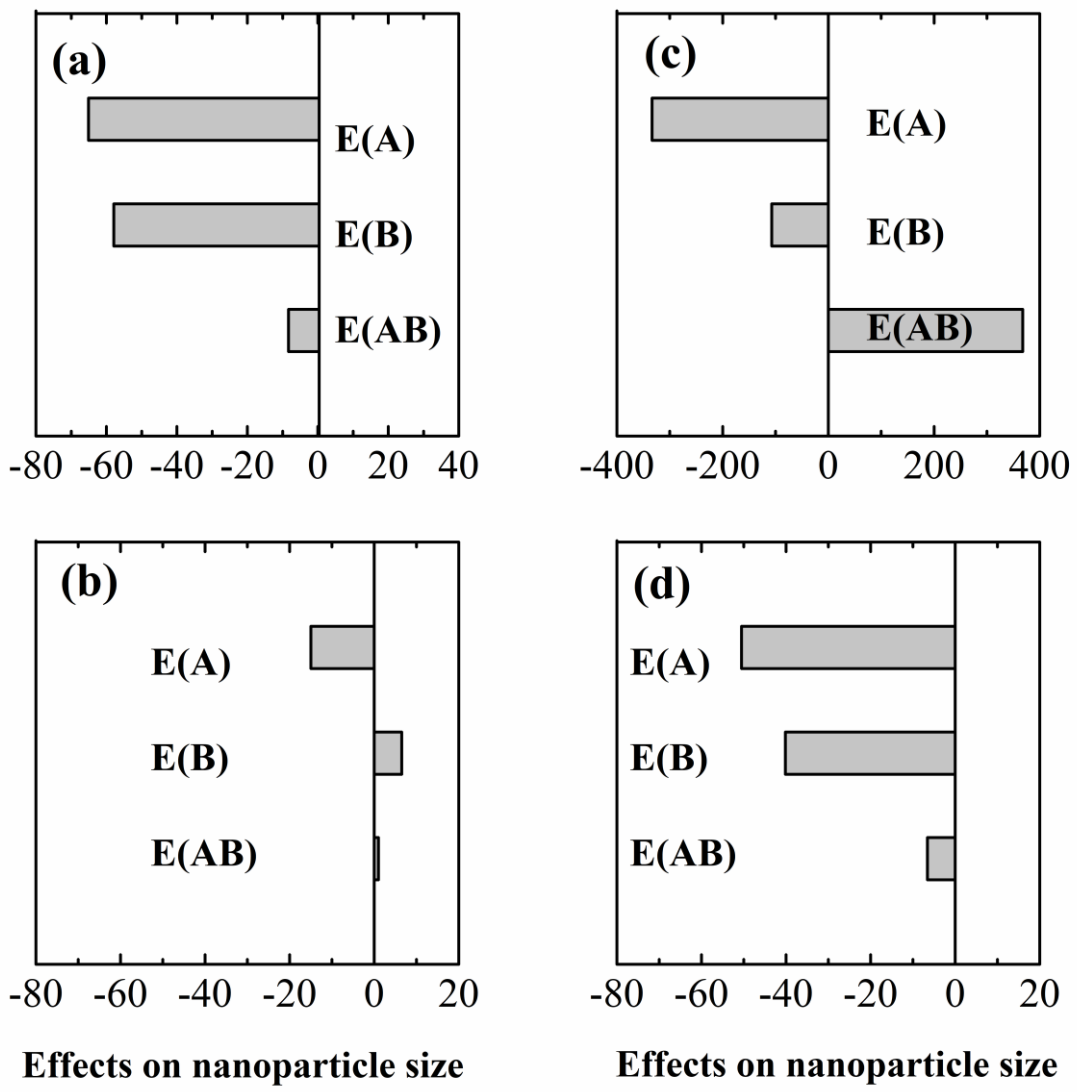
(a)
E(A)
E(B)
E(AB)
-80 -60 -40 -20 0 20 40
(c)
E(A)
E(B)
E(AB)
-400 -200 0 200 400
(b)
E(A)
E(B)
E(AB)
-80 -60 -40 -20 0 20
(d)
E(A)
E(B)
E(AB)
-80 -60 -40 -20 0 20
Effects on nanoparticle size
Effects on nanoparticle size

Figure 9

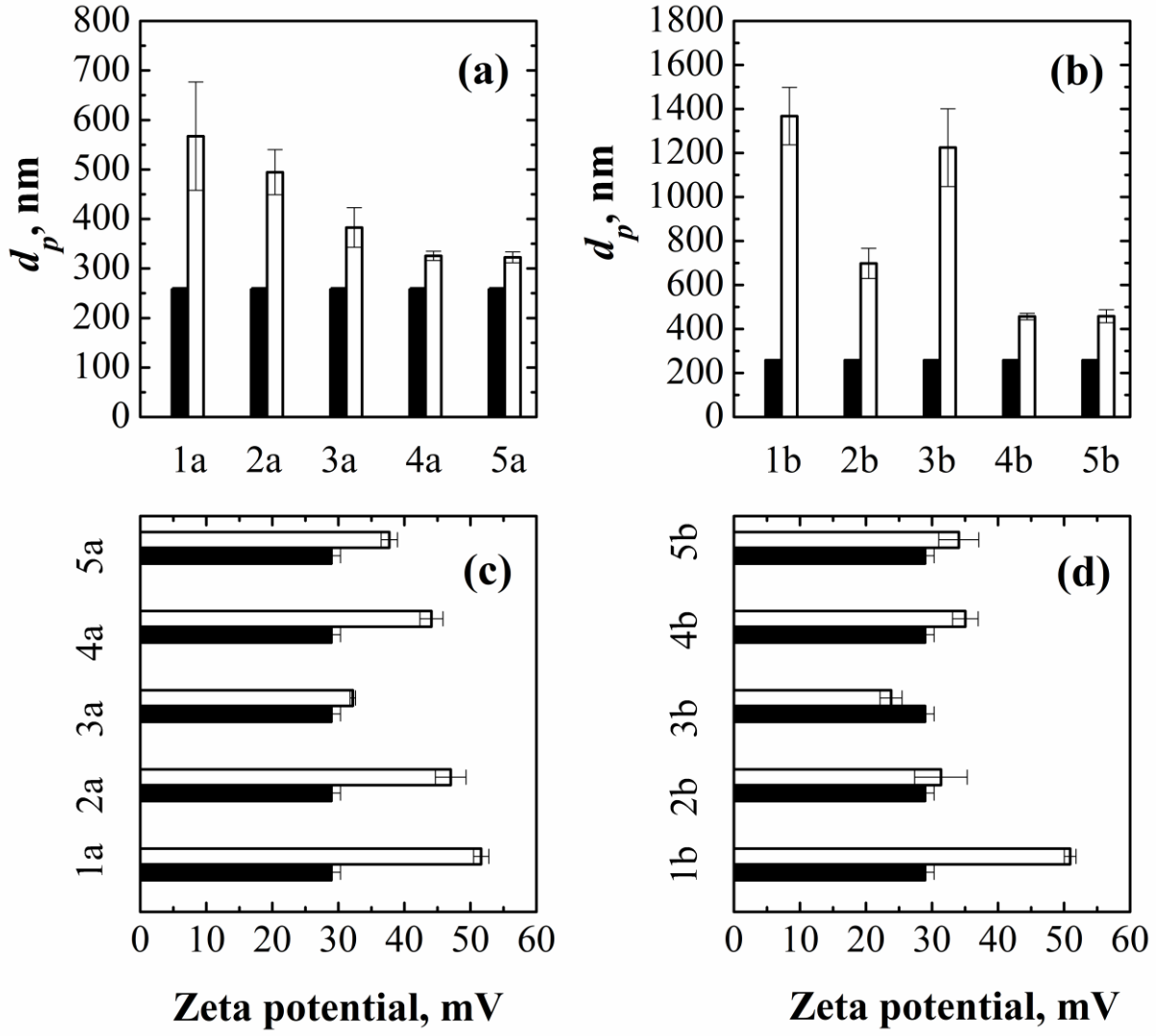

Figure 10

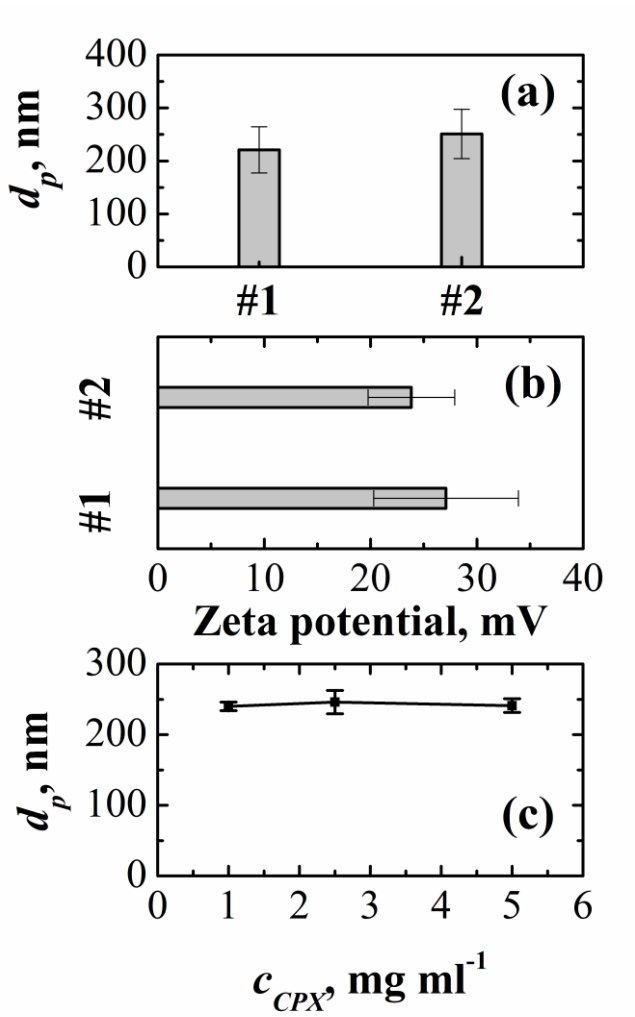
(a)
d_p, nm
400
300
200
100
0
#1
#2
(b)
#2
#1
0
10
20
30
40
Zeta potential, mV
(c)
d_p, nm
300
200
100
0
0
1
2
3
4
5
6
c_{CPX}, mg ml^{-1}